A Brief Climatology of Vertical Wind Variability in the Troposphere and Stratosphere as Seen by the Poker Flat, Alaska, MST Radar

G. D. NASTROM

Control Data Corporation, Minneapolis, MN 55440

K. S. GAGE

Aeronomy Laboratory, National Oceanic and Atmospheric Administration, Boulder, CO 80303

(Manuscript received 9 May 1983, in final form 6 October 1983)

ABSTRACT

A statistical analysis of vertical air motion has been performed for data taken in the 3–20 km altitude range by the Poker Flat MST radar during the period September 1979–January 1982. The variability of vertical velocities is analyzed as a function of season, time of day and synoptic weather conditions. The overall frequency distribution of vertical velocities can be approximated by the sum of two normal distributions: one with variance about 10 times larger than the other. The variability of vertical velocity at all levels is found to correlate most closely with horizontal wind speed at 700 mb on a day-to-day basis. The total variance is larger in summer than in winter at all hours of the day and especially during the afternoon hours. A statistically significant diurnal variation of vertical motions is found during summer with amplitude in the midtroposphere near 2 cm s^{-1}. Interpreting the vertical wind variability as a manifestation of vertically propagating waves, we compare the results here with earlier studies of turbulence variations. These comparisons show a plausible link between the intensity of turbulence at jet stream altitudes and the production of waves near the surface.

1. Introduction

Vertical wind variability in the free atmosphere has only recently become observable over a broad range of scales. While several methods have been used in the past to measure vertical motions on an experimental basis (e.g., aircraft, constant-level balloons, parachutes), each of these methods is presently impractical for widespread or continuous use or lacks the sensitivity required to resolve small-scale motions. With the development of sensitive Doppler radars capable of detecting signals from irregularities of the refractive index in clear air, it has become possible to measure, among other things, the vertical velocity of the air, on a nearly continuous basis. As reviewed by Gage and Balsley (1978) and James (1980), there are several MST (mesosphere–stratosphere–troposphere) radars in operation over the globe, and a number of important results on vertical motions have already been presented (Woodman and Guillen, 1974; Fukao *et al.*, 1978; Peterson and Balsley, 1979; Ecklund *et al.*, 1981, 1982; Gage *et al.*, 1981; Röttger and Schmidt, 1981; Larsen *et al.*, 1982). However, each of these papers has dealt with only a relatively short period of observations, as case studies. The MST radar at Poker Flat, Alaska, (Balsley *et al.*, 1979) has been operating on a quasi-continuous basis since September 1979, and enough data have now been collected to support a statistical analysis of the variability of vertical velocities. Accordingly, in Section 3 of this paper we present a brief statistical summary of vertical wind variability at Poker Flat.

Ecklund *et al.* (1981, 1982) have interpreted the vertical wind variability as a measure of gravity wave activity. They found a notable positive correlation between vertical wind variability, wind and wind shear. Since it has long been thought that the occurrence of clear air turbulence in the free atmosphere is associated with the attenuation of vertically propagating waves, in Section 4 we test this idea by comparing the intensity of turbulence in terms of C_n^2, the refractivity turbulence structure constant (Nastrom *et al.*, 1982), with the vertical wind variability.

2. Vertical wind data

The Poker Flat MST radar is located at 65.13°N, 147.46°W about 40 km north of Fairbanks, Alaska. The basic principles of operation and system description have been given by Balsley *et al.* (1979, 1980), so are not repeated in detail here. Observations are automatically recorded on tape at prescribed time intervals. Winds and other variables are measured at about 2.2 km height intervals centered from 3.8 km to over 20 km. The lower limit is a function of the radar operating parameters, and the upper limit results only from the decreasing signal-to-noise ratio of the echoes. The period of record available for this study is 11 September 1979 through 27 January 1982. As shown in Fig. 1, some data are available every month except for 10 July–28 September 1981. The radar operates quasi-continuously, so the average time interval between observations is approximately inversely proportional to the number of observations per month. However, the number of observations each month is affected by the number of days the radar was operational and by the sampling strategy used (e.g., only vertical winds observed versus both vertical and horizontal winds). Only vertical winds were observed during September 1979–March 1980.

Sample days of vertical wind measurements (Ecklund *et al.*, 1981) at Poker Flat, Alaska, are reproduced in Fig. 2. These figures illustrate the extremes found on quiet and active days, respectively. It is this "duality" of the vertical wind variability which is seen in the next section to dominate the overall statistical distribution of vertical wind variability.

All radar data presented here were supplied by the Aeronomy Laboratory, NOAA, on magnetic tape. A quality control algorithm based on the signal-to-noise ratio was used to eliminate most spurious echoes. Next, for each three-hour interval at each altitude, the mean and standard deviation of velocity were computed, and all velocities over 2.5 standard deviations from the mean were discarded. Finally, time series of the data were edited by visual inspection. These procedures undoubtedly led to a relatively few legitimate observations being discarded, but, more importantly, only a few spurious observations should have survived. Of course, a systematic bias would occur in the vertical wind measurement if the radar beam were tilted off-vertical. In that case there would be a clear relation between variations in horizontal and vertical winds but analysis of monthly mean values shows no clear evidence that this effect is present.

NMC gridded analyses of horizontal winds through 1980 at standard pressure levels, 1000–100 mb, were obtained from NCAR for 00 GMT and 12 GMT each day and are used for comparison purposes. The methods used to produce these analyses are discussed by Kistler and Parrish (1982). MST radar horizontal winds were not available for the entire period of record, so NMC analyses of horizontal winds are used.

3. Vertical wind variability

a. Gross features

The gross features of vertical wind variability can be illustrated succinctly by examining the cumulative frequency distribution in Fig. 3. The cumulative frequency distribution of vertical velocity is plotted here in probability coordinates using all available data below 20 km. The labels on the ordinate apply for the 3.8 km curve, and the curve for each higher altitude, labelled at the left end of the curve, is offset by 10 cm s^{-1}. The usual meteorological convention, that upward motions are positive, is used. The standard deviation (σ, cm s^{-1}) is given near the center of each curve. Vinnichenko *et al.* (1973) report that balloon data below 9 km show that σ is fairly constant with altitude. Their findings are verified and extended by the new results in Fig. 3. The larger σ at 3.8 km may be terrain induced or may partly arise because the radar data at this lowest altitude are compromised at times. Relatively large values of σ at 3.8 km for 3 h intervals will be seen later in Fig. 5. The number of observations, given at the right end of each curve, is fairly constant below about 15 km and then steadily decreases at high altitudes. The number of observations above 15 km will increase greatly with future data as the antenna size and power of the radar were upgraded during the summer of 1981. For example, at the next higher level, 21.2 km (not shown), 41 450 of the 57 000 observations available for this study were taken after September 1981.

The probability coordinates used in Fig. 3 are designed so that a normal (Gaussian) distribution will appear as a straight line. The slope of the line is directly related to the standard deviation and the 50 percentile

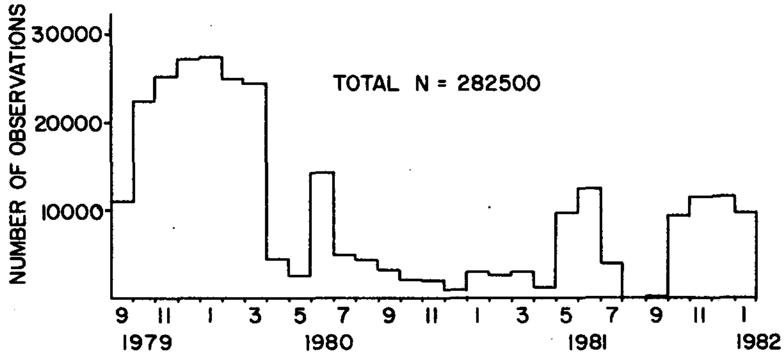

FIG. 1. Number of observations by month of vertical velocity at 6.0 km from the MST radar at Poker Flat, Alaska.

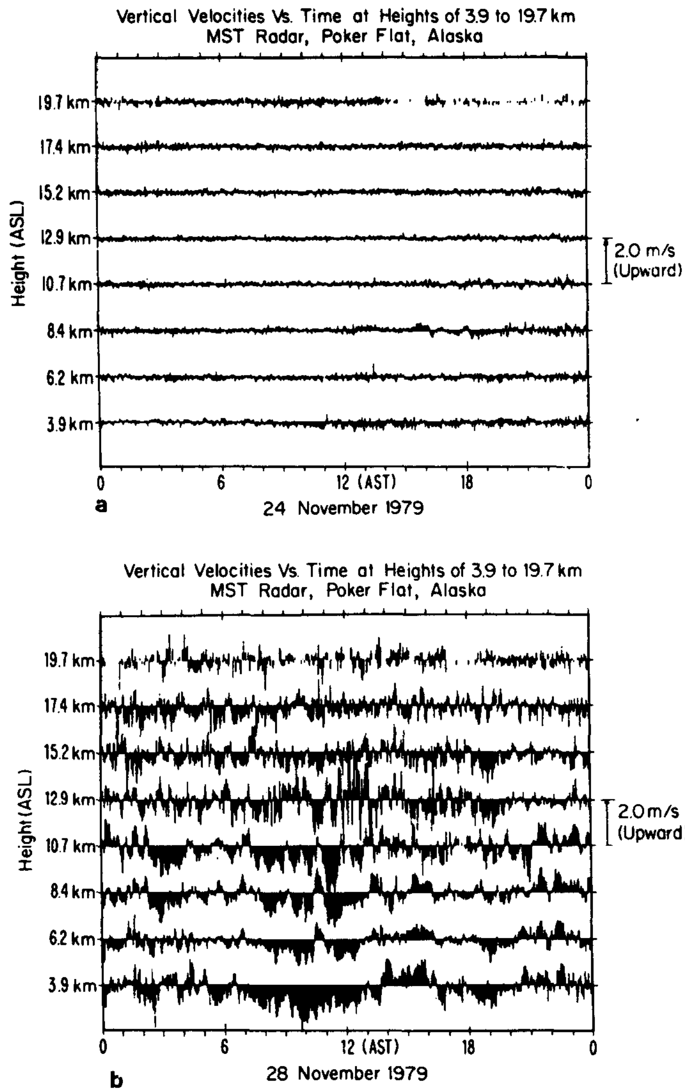

FIG. 2. Vertical velocities on (a) quiet day (24 November 1979) and (b) active day (28 November 1979) (after Ecklund *et al.*, 1981).

value (the median) is equivalent to the mean for a normal distribution. The curves in Fig. 3 are not straight lines, but rather "curl up" at the ends, indicating that extreme winds are observed more often than would be expected for a normal distribution. However, the observed distributions can be approximated as the sum of two Gaussians, associated with quiet and active periods, as discussed next.

The observed frequency distribution at 6.0 km is shown in a routine histogram format in the upper panel of Fig. 4. Also shown in the upper panel is a Gaussian which fairly well matches the wings of the observed distribution. The parameters for the Gaussian were estimated by drawing asymptotes to each end of the curve for 6.0 km in Fig. 3; the standard deviation (σ) is determined from the average slope of the two asymptotes and the mean is from their average intercept with the 50 percentile line. The "number of data" for the Gaussian (N = 43 500) is the portion of the total number that is under the curve. The difference between the two curves in the upper panel of Fig. 4 is shown by the piecewise curve in the lower panel, along with a Gaussian which approximates it. Parameters for the Gaussian in the lower panel were estimated by plotting the data for the piecewise curve in probability coordinates and reading the slope and 50 percentile intercept from the graph (not shown). While this graphical method for fitting two Gaussians to the observed frequency distribution is crude and perhaps not unique, it illustrates the point that there are two separate processes represented in the vertical velocity data.

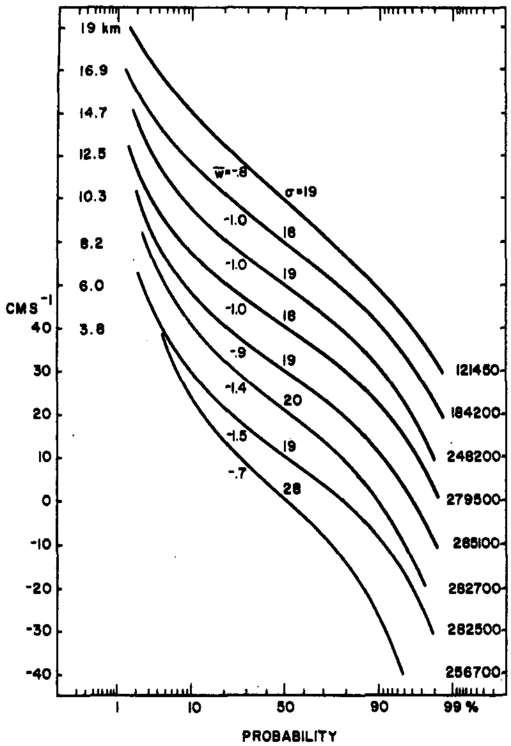

FIG. 3. Cumulative frequency distribution in probability coordinates of vertical velocity. Values on the ordinate apply for the 3.8 km curve, each higher altitude is offset 10 cm s^{-1}. Mean ($\bar{w}$, cm s^{-1}) and standard deviation (σ, cm s^{-1}) are given at the center of each curve.

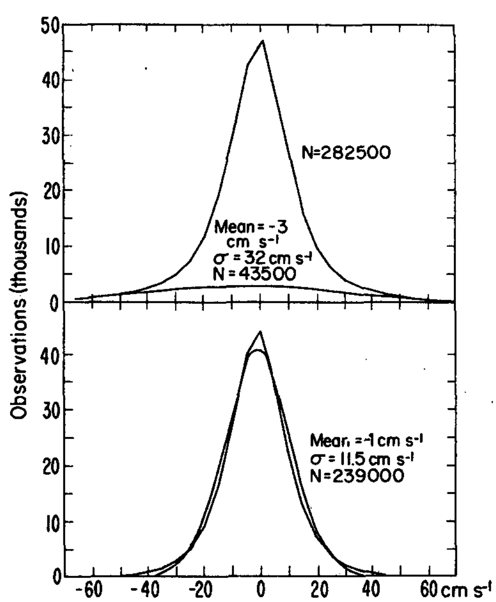

FIG. 4. Illustration of decomposition of observed frequency distribution into two Gaussians. Upper: Frequency distribution of vertical velocities at 6.0 km (piecewise curve), and the Gaussian distribution fit to extremes of the observed values (smooth curve). Lower: Difference between the two curves in the upper panel (piecewise curve), and the Gaussian distribution fit to it (smooth curve).

Most of the time, the vertical velocity variations are fairly small, with an average standard deviation near 10 cm s^{-1} (σ = 11.5 for the Gaussian in the lower panel of Fig. 4). Superposed on this background variability are brief episodes of large activity when the standard deviation increases dramatically (σ = 32 for the upper Gaussian in Fig. 4). Two separate regimes are in fact observed as illustrated in Fig. 2 and in Fig. 5 by the time series plots of standard deviation of vertical velocity over three-hourly intervals during January 1980. That is, above 5 km, $\sigma \leqslant 10$ cm s^{-1} except for periods of large σ near the 9th, 19th, and 29th.

It is interesting that the episodes of enhanced standard deviation seem to start simultaneously at all levels above 5 km. Ecklund *et al.* (1981) compared vertical wind data with synoptic weather maps and tentatively attributed the periods of enhanced vertical wind variability to enhanced gravity wave activity associated with the passage of storms or jet streams. In the present study this connection can be seen by the correlation between horizontal wind speed and vertical wind variability in Fig. 5. The simultaneous occurrence of wave activity over a broad range of altitudes may be a consequence of the relatively fast vertical group velocity of gravity waves as compared to the three-hourly time resolution used here.

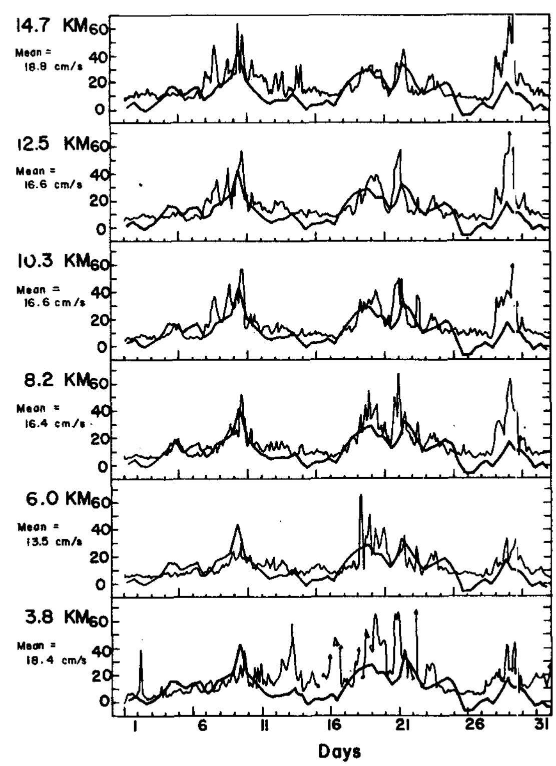

FIG. 5. Time series of the standard deviations of vertical velocity over three-hourly intervals during January 1980. The bold line plotted is the 700 mb horizontal wind speed (relative units).

b. Day-to-day variations

Day-to-day changes in vertical wind variability during winter are illustrated in Fig. 5. Also shown in Fig. 5 are the horizontal wind speeds at 700 mb (3.0 km in the standard atmosphere) from NMC analyses. Note the close relation of vertical wind variability to the 700 mb wind. A similar relationship was found at Platteville, Colorado by Ecklund *et al.* (1982). The relationship between horizontal wind speed and standard deviation of vertical velocity is summarized in Fig. 6 by profiles of correlation coefficients. The number of data pairs at each height is about 750 so that correlations above 0.15, assuming only ½ the pairs are independent, are significant at the 1% level by Student's *t* test. Not all data pairs are independent due to temporal autocorrelation of the wind and vertical velocity as discussed elsewhere (Nastrom and Gage, 1983). Above 5 km, vertical velocity standard deviation at Poker Flat at all heights correlates best with the 700 mb wind speed.

We have also examined the correlation between vertical wind variability and the vertical shear of the horizontal wind. The magnitude of vector shear, i.e., the magnitude of the wind difference across the layer 850–300 mb, is used in Fig. 6 for illustration, although shears over other layers and height scales give similar low correlations. While vertical shear of horizontal winds appears to be a relatively poor indicator of vertical velocity activity during the long-time span used here (September 1979–December 1980), high resolution shear data, had they been available, might have shown a much better correlation. Certainly, this would have to be the case if the gravity waves are generated

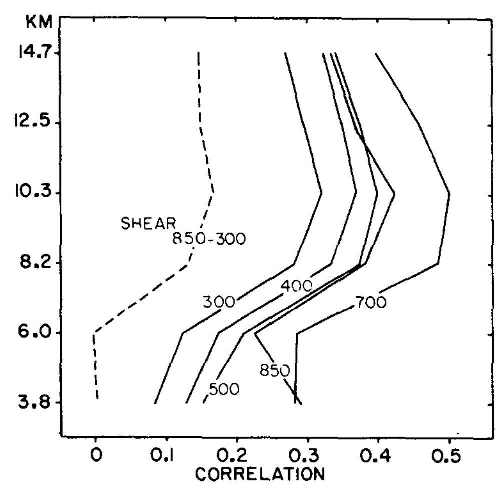

FIG. 6. Correlation of standard deviation of vertical velocity (over three-hourly intervals centered near 0000 and 1200 GMT) as a function of height with horizontal wind speed from NMC analyses at the pressure level indicated along each curve. Also, correlation with vector shear across the layer 850 mb (1.5 km) to 300 mb (9.1 km). Period of record is September 1979–December 1980.

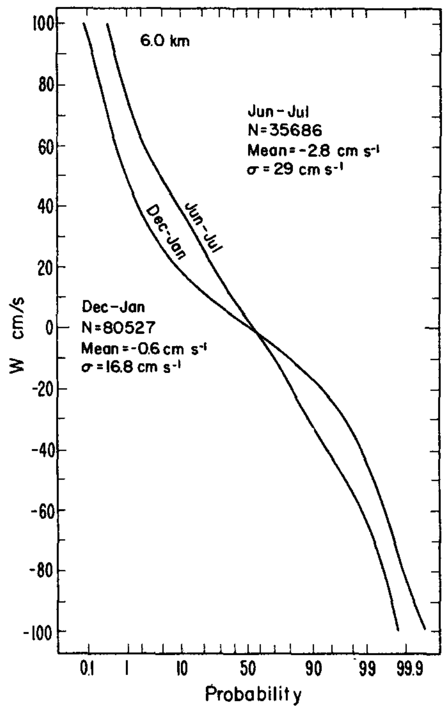

FIG. 7. Cumulative frequency distribution at 6.0 km in probability coordinates during summer and winter.

primarily by shear instability. However, if flow over rough terrain is the primary wave source, the horizontal wind speed at terrain height would be highly correlated with wave activity. While at first glance the results of Figs. 5 and 6 seem more consistent with a surface source of gravity waves than with a jet stream source of waves, definition of the generating mechanism remains an open issue.

c. Seasonal and diurnal variations

Cumulative frequency distributions of vertical velocity at 6 km are compared in Fig. 7 for summer (June–July) and winter (December–January). Note that the summer distribution is nearly a straight line except for 1–2% of the observations in the extreme tails of the curve. The primary source of variability in summer is likely associated with convective activity as discussed later. In contrast the winter curve "curls up" much sooner near the ends and asymptotically become parallel to the summer curves only in the extreme tails. Thus, as found in Fig. 4, the winter curve is the sum of two distributions: a quiet-time one with relatively small variability and an active-time one associated with periods of strong winds.

Seasonal changes of the standard deviation are shown in detail in Fig. 8 by the time series of monthly values at 6 and 12.5 km. Not only is the average magnitude of the standard deviation similar among altitude levels (consistent with the long-term values given in

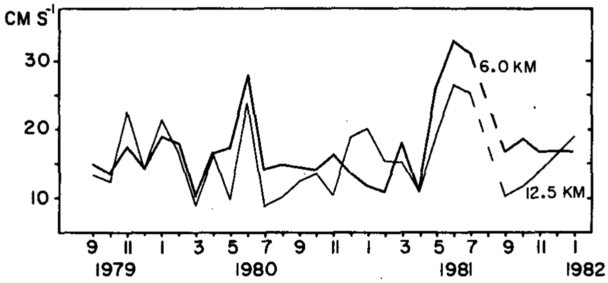

FIG. 8. Standard deviation of vertical velocity at 6.0 and 12.5 km by month.

Fig. 3), but also the detailed changes from month to month are fairly well correlated. The correlation of three-hourly standard deviations was noted in Fig. 5. Since the correlation of changes in five-minute data has already been demonstrated by Ecklund *et al.* (1982), we conclude that changes in vertical wind variability are correlated on time scales from minutes to months over broad height intervals in the troposphere and stratosphere.

Another feature evident in Fig. 8 is the appearance of large vertical wind variability in the period of maximum local insolation (June and July). If this feature were due to the predominance of convective activity during the time of maximum insolation, we might also expect to see a diurnal variation in vertical wind variability at this time of year. Fig. 9 shows changes with

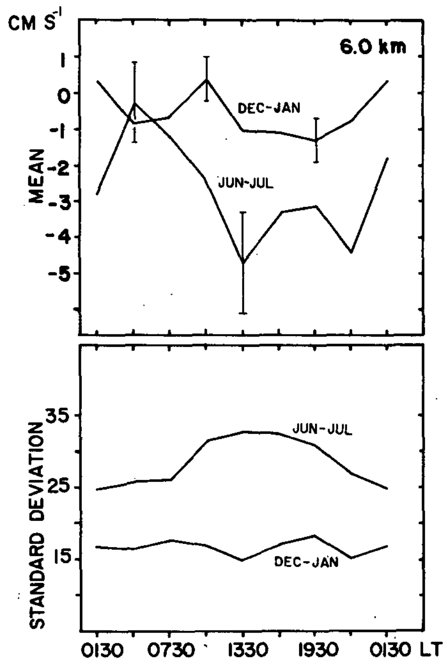

FIG. 9. Diurnal variation during summer and winter at 6 km. Statistical error bars in the upper panel correspond to 95% confidence limits, after adjustment for autocorrelation of the data.

time of day of the mean (upper panel) and standard deviation (lower panel) of vertical velocity at 6 km during summer and winter. Except for the three-hourly interval centered at 0430 Local Standard Time (LT), the magnitude of the means during summer are always larger than during winter. Also, in Fig. 9 the standard deviation during summer is always larger than during winter, especially during late morning and afternoon hours. (Diurnal changes of standard deviation decrease with altitude, and the lower stratosphere standard deviation is not a function of time of day.) Statistical error bars in the upper panel extend two times the standard error of the mean (SE) above and below the mean values to represent the 95% confidence limits of the means, where SE is given by

$$SE = \sigma/\sqrt{N'}. \tag{1}$$

σ is the standard deviation and N' is the number of independent observations used, after adjustment for autocorrelation. The standard statistical Student's t test indicates that the daily maxima and minima are different at the 1% confidence level in both summer and winter. Thus, there is a statistically significant diurnal variation, but note that both summer and winter means show two maxima per day, suggesting that a semidiurnal component is also present. To resolve the diurnal and semidiurnal components, a harmonic analysis of the 3 h means was made and the results are given in Table 1. For both waves the largest amplitudes are found in the troposphere during summer.

It seems unlikely that these waves are related to the global-scale diurnal and semidiurnal tides as their magnitudes are about two orders of magnitude larger and their phase bears little resemblance to theoretical prediction (Lindzen, 1967; Lindzen and Hong, 1974). Rather, they are likely induced by local terrain and differential heating.

TABLE 1. Amplitude and phase (time of maximum downward speed) of diurnal and semidiurnal oscillations.

	Summer		Winter	
	Amplitude (cm s^{-1})	Phase (LT)	Amplitude (cm s^{-1})	Phase (LT)
Diurnal				
3.8 km	2.8	1530	1.5	0930
6.0	1.4	1800	0.2	1430
8.2	1.2	2400	0.7	1200
10.3	0.5	0800	0.3	0630
12.5	0.1	1300	0.2	2330
14.7	0.4	1900	0.5	1600
Semidiurnal				
3.8 km	1.4	1215	0.5	1400
6.0	1.0	1200	0.2	0600
8.2	0.7	0845	0.7	0500
10.3	0.2	1430	0.1	0700
12.5	0.1	1445	0.3	1000
14.7	0.1	0430	0.2	0500

Slope and valley wind circulation systems are discussed in detail by Atkinson (1981). These circulation systems arise from differential heating in valleys and surrounding sloping terrain. Since they are thermally driven, they have a clear diurnal variation and also vary with season. While these circulations have maximum amplitudes in the boundary layer, their influence can extend to midtropospheric altitudes.

The vertical and seasonal variation of the diurnal oscillation of the vertical motion observed by the Poker Flat radar is summarized in Fig. 10. A clear decrease in amplitude of the diurnal oscillation with increasing altitude is evident. Also, as expected, the amplitude is greatest during the season of maximum insolation. The fact that the Poker Flat radar is located in a river valley with nearby southward facing hill slopes supports this interpretation.

4. A comparison of vertical wind variability and turbulence variations

It has long been recognized that vertically propagating internal gravity waves act to couple the lower and upper atmospheres. In particular, it is thought that waves generated in the lower atmosphere play an important role in the generation of clear air turbulence (Bretherton, 1969; VanZandt *et al.*, 1981). If we interpret the vertical wind variability as an indicator of gravity wave activity, we can explore the connection between wave activity and turbulence, as measured by C_n^2 (Gage *et al.*, 1980; Weinstock, 1981). A preliminary climatology of C_n^2 has been prepared using Poker Flat MST radar data (Nastrom *et al.*, 1981, 1982), and these results will be used for qualitative comparisons

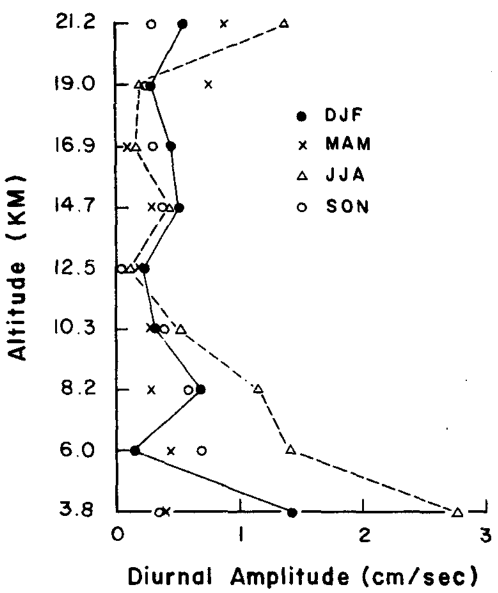

FIG. 10. Vertical profiles of the amplitude of the diurnal oscillation showing seasonal variation.

below. A more complete analysis of the C_n^2 variations using an improved data set is in progress and should give results suitable for more detailed comparisons in the near future.

A comparison of the behavior of vertical wind variability and C_n^2 shows many common features. The most obvious connection between these two quantities is their positive correlation with wind speed. However, vertical wind variability is best correlated with the lower tropospheric wind (at 700 mb) while C_n^2 is best correlated with the wind near the tropopause level (Nastrom *et al.*, 1981, and Smith *et al.*, 1983). This difference in behavior may be related to the fact that waves appear to be generated primarily in the lower troposphere and are Doppler shifted as they propagate vertically while clear air turbulence and hence C_n^2 variations are most pronounced in the lower stratosphere in regions of strong shear associated with jet streams where critical layer interactions are expected.

Seasonal and diurnal variations of vertical wind variability and C_n^2 also have much in common. Both vertical wind variability and C_n^2 are generally higher near the time of maximum insolation. This supports the idea that convection in the troposphere is an important source of gravity waves.

5. Summary and conclusions

Analyses of the large body of vertical velocity measurements from MST radar data at Poker Flat, Alaska, have been used to describe the main regimes of variability of vertical velocity, 3–20 km. The frequency distribution of velocities is nearly symmetric, and can be represented by the sum of two normal (Gaussian) distributions. During summer a single normal distribution matches the observed distribution fairly well. It is suggested that the large variance process during winter arises from enhanced gravity wave activity in baroclinic storms. The standard deviation of vertical velocity at Poker Flat is most closely correlated with horizontal wind speed at 700 mb. There is a statistically significant diurnal variation in mean vertical velocity both in summer and winter, which likely arises from convective activity and local terrain effects. These features of vertical wind variability have much in common with the variations of turbulence intensity found in radar measurements of C_n^2. A comparison of the variations of vertical wind variability and turbulence demonstrates a reasonable consistency with the idea that the vertical wind variability is a measure of wave activity and that the waves propagate vertically to produce clear air turbulence.

The climatological results presented here should help provide a framework within which to interpret results from the case studies noted earlier and from future studies using vertical velocity data. They will also prove valuable in a related study in progress assessing the relation between synoptic scale vertical velocities and those measured using the radar technique. Only variations with time and height have been studied here; it is important to stress the need for collecting similar data sets in other geographical areas to determine any variation that may occur with terrain or latitude.

Acknowledgments. We gratefully acknowledge the contributions of Ben Balsley, Warner Ecklund and Anthony Riddle of NOAA's Aeronomy Laboratory, both for supplying the radar data and for many helpful discussions. This research was supported in part by the Air Force Office of Scientific Research. The Poker Flat MST Radar is partially supported by the Atmospheric Sciences Section of the National Science Foundation.

REFERENCES

Atkinson, B. W., 1981: *Meso-Scale Atmospheric Circulations*. Academic Press, Chapt. 6.

Balsley, B. B., W. L. Ecklund, D. A. Carter and P. E. Johnston, 1979: The Poker Flat MST radar: First results. *Geophys. Res. Lett.*, **6**, 921–924.

——, ——, —— and ——, 1980: The MST radar at Poker Flat, Alaska. *Radio Sci.*, **15**, 213–223.

Bretherton, F. P., 1969: Waves and turbulence in stably stratified fluids. *Radio Sci.*, **4**, 1279–1287.

Ecklund, W. L., K. S. Gage, and A. C. Riddle, 1981: Gravity wave activity in vertical winds observed by the Poker Flat MST radar. *Geophys. Res. Lett.*, **8**, 285–288.

——, ——, B. B. Balsley, R. G. Strauch and J. L. Green, 1982: Vertical wind variability observed by VHF radar in the lee of the Colorado Rockies. *Mon. Wea. Rev.*, **110**, 1451–1457.

Fukao, S., S. Kato, S. Yokoi, R. M. Harper, R. F. Woodman and W. E. Gordon, 1978: One full-day radar measurement of lower stratosphere winds over Jicamarca. *J. Atmos. Terr. Phys.*, **40**, 1331–1338.

Gage, K. S., and B. B. Balsley, 1978: Doppler radar probing of the clear atmosphere. *Bull. Amer. Meteor. Soc.*, **58**, 1074–1093.

——, J. L. Green and T. E. VanZandt, 1980: Use of Doppler radar for the measurement of atmospheric turbulence parameters from the intensity of clear-air echoes. *Radio Sci.*, **15**, 407–416.

——, D. A. Carter and W. L. Ecklund, 1981: The effect of gravity waves on specular echoes observed by the Poker Flat MST radar. *Geophys. Res. Lett.*, **8**, 599–602.

James, P. K., 1980: A review of radar observations of the troposphere in clear air conditions. *Radio Sci.*, **15**, 151–174.

Kistler, R. E., and D. F. Parrish, 1982: Evolution of the NMC data assimilation system: September 1978–January 1982. *Mon. Wea. Rev.*, **110**, 1335–1346.

Larsen, M. F., W. E. Swartz and R. F. Woodman, 1982: Gravity-wave generation by thunderstorms observed with a vertically-pointing 430 MHz radar. *Geophys. Res. Lett.*, **9**, 571–574.

Lindzen, R. S., 1967: Thermally driven diurnal tide in the atmosphere. *Quart. J. Roy. Meteor. Soc.*, **93**, 18–42.

——, and S. Hong, 1974: Effects of mean winds and horizontal temperature gradients on solar and lunar semidiurnal tides in the atmosphere. *J. Atmos. Sci.*, **31**, 1421–1446.

Nastrom, G. D., and K. S. Gage, 1983: A brief climatology of vertical air motions from MST radar data at Poker Flat, Alaska. *Preprints 21st Conf. on Radar Meteorology*, Edmonton, Amer. Meteor. Soc., 135–140.

—— B. B. Balsley and K. S. Gage, 1981: Changes with season of C_n^2 at Poker Flat, Alaska, from MST Doppler radar observations. *Preprints 20th Conf. on Radar Meteorology*, Boston, Amer. Meteor. Soc., 136–141.

——, K. S. Gage and B. B. Balsley, 1982: Variability of C_n^2 at Poker Flat, Alaska, from mesosphere, stratosphere, troposphere (MST) Doppler radar observations. *Opt. Eng.*, **21**, 347–351.

Peterson, V. L., and B. B. Balsley, 1979: Clear air Doppler radar measurements of the vertical component of wind velocity in the troposphere and stratosphere. *Geophys. Res. Lett.*, **6**, 933–936.

Röttger, J., and G. Schmidt, 1981: Characteristics of frontal zones determined from spaced antenna VHF radar observations. *Preprints 20th Conf. Radar Meteorology*, Boston, Amer. Meteor. Soc., 30–37.

Smith, S. A., G. J. Romick and K. Jayaweera, 1983: Poker Flat MST radar observations of shear induced turbulence. *J. Geophys. Res.*, **88**, 5265–5271.

VanZandt, T. E., K. S. Gage and J. M. Warnock, 1981: An improved model for the calculation of profiles of C_n^2 and ϵ in the free atmosphere from background profiles of wind, temperature, and humidity. *Preprints 20th Conf. Radar Meteorology*, Boston, Amer. Meteor. Soc., 129–135.

Vinnichenko, N. K., N. Z. Pinus, S. M. Schmeter and G. N. Shur, 1973: Turbulence in the free atmosphere. Translation by Consultants Bureau, 263 pp.

Weinstock, J., 1981: Using radar to estimate dissipation rates in thin layers of turbulence. *Radio Sci.*, **16**, 1401–1406.

Woodman, R. F., and A. Guillen, 1974: Radar observations of winds and turbulence in the stratosphere and mesosphere. *J. Atmos. Sci.*, **31**, 493–505.